Proc. Estonian Acad. Sci. Phys. Math., 1999, **48**, 3/4, 252–264
https://doi.org/10.3176/phys.math.1999.3/4.08

NONLINEAR INTERACTION OF LONGITUDINAL WAVES IN ELASTIC MATERIAL

Arvi RAVASOO and Andres BRAUNBRÜCK

Department of Mechanics and Applied Mathematics, Institute of Cybernetics, Tallinn Technical University, Akadeemia tee 21, 12618 Tallinn, Estonia; arvi@ioc.ee

Received 16 February 1999

Abstract. Nonlinear interaction of longitudinal waves in elastic material with nonlinear physical properties is investigated theoretically. The analytical solution to describe the propagation of two longitudinal waves excited simultaneously on the parallel opposite surfaces of the material is derived. The one-dimensional nonlinear propagation and interaction of sine waves are studied in detail. The peculiarities of the evolution and interaction of nonlinear effects that accompany sine-wave propagation and reflection are clarified on the basis of numerical simulation data.

Key words: longitudinal waves, elastic material, nonlinearity, interaction.

1. INTRODUCTION

Most ultrasonic nondestructive testing (NDT) methods of materials [1–3] are based on the analyses of one-directional wave propagation. The data available from these studies are insufficient for determining the properties of inhomogeneous materials, thus it is necessary to enhance the efficiency of NDT. With this aim the utilization of nonlinear effects of one-directional wave propagation in NDT of materials has been proposed [4,5]. Consideration of the wave interaction process in NDT of materials with complicated properties will also augment information in this field.

Nonlinear propagation, reflection, and interaction of longitudinal waves have been intensively investigated for a long time. Different asymptotic approaches have been used to describe velocity variation and profile distortion of nonlinear waves during these processes (see, e.g., [6,7] and references therein).

In this paper the simultaneous nonlinear propagation of two longitudinal waves is studied, following the requirements of NDT. Waves are excited on the opposite surfaces of the material (structural element) in terms of particle velocity and recorded on the same surfaces in terms of stress. This process is described by the analytical asymptotic solution of the nonlinear wave equation which permits us to investigate the propagation of waves with an arbitrary smooth initial profile.

The nonlinear propagation, reflection, and interaction of sine waves are studied in detail. Analytical expressions to describe simultaneous propagation of two sine waves are derived and on the basis of these cumbersome expressions illustrative plots are computed. These plots enable us to analyse the possibility of using data on sine wave profile evolution and velocity variation in NDT of nonlinear elastic materials. The results presented in this paper may be regarded as reference data for the development of procedures for NDT of materials with complicated properties.

2. ELASTIC MATERIAL DYNAMICS

The dynamics of isotropic and homogeneous nonlinear elastic material is described by the nonlinear theory of elasticity. The equation of motion of the material is expressed in Lagrangian rectangular coordinates X_K in the form [8]

$$\{T_{KL}(X_J,t)[\delta_{KL}+U_{k,L}(X_J,t)]\}_{,K}-\rho U_{k,tt}(X_J,t)=0, \tag{1}$$

where $U_k(X_J,t)$ is the displacement vector, $T_{KL}(X_J,t)$ is the Kirchhoff pseudo-stress tensor, δ_{KL} is the Kronecker delta, and ρ is the material density. The indices after the comma, K, k, and t, indicate differentiation with respect to Lagrangian rectangular coordinates X_K, Eulerian rectangular coordinates x_k, or the time t, respectively. Here, the usual summation convention is used and all indices run over 1, 2, 3. Equation (1) takes the physical and geometrical nonlinearity into account.

In this paper attention is confined to the one-dimensional problem of nonlinear longitudinal wave propagation along the $X_1 \equiv X$ axis. Dynamics of the material is governed by the equation of motion derived from (1)

$$[1+k_1U_{,X}(X,t)]U_{,XX}(X,t)-c^{-2}U_{,tt}(X,t)=0. \tag{2}$$

The coefficients of (2),

$$k_1=3[1+2k_0(\nu_1+\nu_2+\nu_3)], \qquad c^2=(k_0\rho)^{-1}, \qquad k_0=(\lambda+2\mu)^{-1}, \tag{3}$$

are functions of the material density ρ, the Lamé coefficients λ and μ, and the third-order elastic coefficients ν_1, ν_2, and ν_3. U denotes the displacement vector component U_1 in (2).

It is easy to see that the Lamé coefficients λ and μ and the third-order elastic coefficients ν_1, ν_2, and ν_3 are grouped in coefficients (3) as follows:

$$\begin{aligned} \alpha &= \lambda + 2\mu, \\ \beta &= 2(\nu_1 + \nu_2 + \nu_3). \end{aligned} \tag{4}$$

This means that NDT of material properties on the basis of data on one-dimensional wave propagation cannot determine the Lamé coefficients λ and μ and the third-order elastic coefficients ν_1, ν_2, and ν_3 separately. The linear and nonlinear material properties are characterized by the constants α and β, respectively.

3. LONGITUDINAL WAVES

Two longitudinal waves with arbitrary smooth initial profiles are excited simultaneously on the opposite parallel surfaces of the material. The problem is considered as one-dimensional. The initial stage of the wave profile distortion is investigated. It is supposed that at this initial stage the distortion of the initially smooth wave profiles is weak and the shock waves are not generated.

The propagation, reflection, and interaction of waves are described analytically on the basis of (2), making use of the perturbation theory. The solution to (2) is sought in the form of the series

$$U(X,t) = \sum_{n=1}^{\infty} \varepsilon^n \, U^{(n)}(X,t), \tag{5}$$

where ε is the positive constant that satisfies the condition $\varepsilon \ll 1$.

In one-dimensional formulation waves in the material are excited simultaneously at two points of the X-axis: at the points $X = 0$ and $X = L$. The wave excited at the point $X = 0$ propagates in the positive direction and the wave excited at the point $X = L$ in the negative direction of the X-axis in correspondence with the initial and boundary conditions to Eq. (2)

$$\begin{aligned} U(X,0) &= U_{,t}(X,0) = 0, \\ U_{,t}(0,t) &= \varepsilon \, a_0 \, \varphi(t) \, H(t), \\ U_{,t}(L,t) &= \varepsilon \, a_L \, \psi(t) \, H(t). \end{aligned} \tag{6}$$

Here $H(t)$ denotes the Heaviside function, a_0 and a_L are constants. The functions $\varphi(t)$ and $\psi(t)$ determine the arbitrary and smooth initial wave profiles. They satisfy the conditions $\max \mid \varphi(t) \mid = 1$, $\max \mid \psi(t) \mid = 1$ and ensure that $\lim_{t\to 0} U_{,t}(0,t) = \lim_{t\to 0} U_{,t}(L,t) = 0$ in consonance with the initial conditions.

Following the perturbation procedure, we introduce the series (5) into (2) and, equating to zero the terms of equal power in ε, arrive at

$O(\varepsilon)$:

$$U^{(1)}_{,XX}(X,t) - c^{-2}\, U^{(1)}_{,tt}(X,t) = 0, \tag{7}$$

$O(\varepsilon^2)$:

$$U^{(2)}_{,XX}(X,t) - c^{-2}\, U^{(2)}_{,tt}(X,t) = -k_1\, U^{(1)}_{,X}(X,t)\, U^{(1)}_{,XX}(X,t), \tag{8}$$

$O(\varepsilon^3)$:

$$\begin{aligned} U^{(3)}_{,XX}(X,t) - c^{-2}\, U^{(3)}_{,tt}(X,t) &= \\ -k_1\, [\, U^{(1)}_{,X}(X,t)\, U^{(2)}_{,XX}(X,t) &+ U^{(1)}_{,XX}(X,t)\, U^{(2)}_{,X}(X,t)]. \end{aligned} \tag{9}$$

The first term in the series (5) is the solution of (7) under the initial and boundary conditions

$$\begin{aligned} U^{(1)}(X,0) &= U^{(1)}_{,t}(X,0) = 0, \\ U^{(1)}_{,t}(0,t) &= a_0 \varphi(t) H(t), \\ U^{(1)}_{,t}(L,t) &= a_L \psi(t) H(t). \end{aligned} \tag{10}$$

This solution

$$\begin{aligned} U^{(1)}(X,t) = a_0\, H(\xi) \int_0^{\xi} \varphi(\tau) d\tau + a_L\, H(\eta) \int_0^{\eta} \psi(\tau) d\tau \\ - a_0\, H(\theta) \int_0^{\theta} \varphi(\tau) d\tau - a_L\, H(\zeta) \int_0^{\zeta} \psi(\tau) d\tau, \end{aligned} \tag{11}$$

$$\begin{aligned} \xi &= t - X/c, & \eta &= t - L/c + X/c, \\ \zeta &= t - L/c - X/c, & \theta &= t - 2\,L/c + X/c, \end{aligned}$$

describes simultaneous propagation of two waves in homogeneous isotropic elastic material in the time interval $0 \le t < 2L/c$. The first term in (11) determines the wave excited at the point $X = 0$ that propagates in the positive direction of the X-axis in the domain $0 \le X \le L$. Reflection of this wave from the point $X = L$ is described by the sum of the first and the third term. The third term determines also the further propagation of this wave during the considered time interval. In a similar way, the second term determines the wave excited at the point $X = L$ that propagates in the negative direction of the X-axis. The fourth term, together with the second one, describes the reflection process of this wave from the point $X = 0$ and propagation of this wave after reflection.

The second and the third term in the series (5) can be determined from (8) and (9) under the initial and boundary conditions

$$U^{(n)}(X,0) = U^{(n)}_{,t}(X,0) = U^{(n)}_{,t}(0,t) = U^{(n)}_{,t}(L,t) = 0, \;\; n = 2, 3. \tag{12}$$

It is easy to notice that (8) and (9) may be presented in the unique form

$$U^{(n)}_{,XX}(X,t) - c^{-2}\, U^{(n)}_{,tt}(X,t) = \sum_{j=1}^{m} G^{(n)}_j(X)\, F^{(n)}_j(\vartheta^{(n)}_j), \tag{13}$$

$$\vartheta^{(n)}_j = t - g^{(n)}_j(X), \quad g^{(n)}_j(X) \geq 0,$$

with the known right-hand side where it is possible to separate the independent variables X and $\vartheta^{(n)}_j$.

The Laplace integral transform with respect to time is applied to (13):

$$\begin{aligned} &U^{(n)\,\mathcal{L}}_{,XX}(X,p) - c^{-2}\, p^2\, U^{(n)\,\mathcal{L}}(X,p) \\ &\qquad = \sum_{j=1}^{m} e^{-p\, g^{(n)}_j(X)}\, G^{(n)}_j(X)\; F^{(n)\,\mathcal{L}}_j(p), \end{aligned} \tag{14}$$

where p is the transform parameter and the upper index $\mathcal{L}$ denotes the Laplace integral transform of the corresponding functions.

The second-order inhomogeneous ordinary differential equation (14) has the solution

$$\begin{aligned} &U^{(n)\,\mathcal{L}}(X,p) \\ &\quad = \sum_{j=1}^{m} \left\{ \frac{c}{2p} F^{(n)\,\mathcal{L}}_j(p) \left[P^{(n)}_j(X,p) - e^{-p\,L/c}(V^{(n)}_j(X,p) + W^{(n)}_j(X,p)) \right] \right\}. \end{aligned} \tag{15}$$

Here, the functions $V^{(n)}_j(X,p)$ and $W^{(n)}_j(X,p)$ are given by the expressions

$$V^{(n)}_j(X,p) = e^{p\,(X-L)/c} \left[-\, e^{-p\,L/c} P^{(n)}_j(0,p) + P^{(n)}_j(L,p) \right], \tag{16}$$

$$W^{(n)}_j(X,p) = e^{-p\,(X+L)/c} \left[-\, e^{p\,L/c} P^{(n)}_j(0,p) + P^{(n)}_j(L,p) \right]. \tag{17}$$

The functions $F^{(n)\,\mathcal{L}}_j(p)$ are determined by the initial wave profiles. The functions $P^{(n)}_j(X,p)$ are dependent on the properties of the material, i.e., on the functions $G^{(n)}_j(X)$ and $g^{(n)}_j(X)$:

$$\begin{aligned} P^{(n)}_j(X,p) = e^{-p\,X/c} \Big[& e^{2p\,X/c} \int e^{-p(X/c + g^{(n)}_j(X))}\, G^{(n)}_j(X)\, dX \\ & - \int e^{p(X/c - g^{(n)}_j(X))}\, G^{(n)}_j(X)\, dX \Big]. \end{aligned} \tag{18}$$

Applying the Laplace inverse transform to the expression (15), we get the solution of (13)

$$U^{(n)}(X,t) = \lim_{Y\to\infty} \frac{1}{2\pi i} \int_{\alpha-iY}^{\alpha+iY} e^{tp}\, U^{(n)\,\mathcal{L}}(X,p)\, dp. \tag{19}$$

The solution (19) determines all terms except the first in the series (5) and it is valid in the time interval

$$0 \leq t < 2L/c. \tag{20}$$

The solutions (11) and (19) to the one-dimensional problem (2), (6) describe the propagation, reflection, and interaction of longitudinal waves with arbitrary smooth initial profiles $\varphi(t)$ and $\psi(t)$ in elastic material.

4. SINE WAVE PROPAGATION

The propagation, reflection, and interaction of longitudinal waves in the nonlinear elastic material are studied on the basis of the solution (5) in one-dimensional formulation. The initial profiles of the waves are defined by the sine function

$$\varphi(t) = \sin \omega t\,,\ \psi(t) = \sin \omega t, \tag{21}$$

where ω denotes the frequency.

The wave process in the elastic material is excited in terms of particle velocity. Consequently, it is convenient to analyse the wave propagation on the basis of the solution (5) also in terms of particle velocity:

$$U_{,t}(X,t) = \sum_{n=1}^{\infty} \varepsilon^n\, U_{,t}^{(n)}(X,t). \tag{22}$$

The first term in the solution (22) determined by (11) has the form

$$\varepsilon\, U_{,t}^{(1)}(X,t) = A_0^{(1)} \sin \omega\xi + A_L^{(1)} \sin \omega\eta - A_0^{(1)} \sin \omega\theta - A_L^{(1)} \sin \omega\zeta, \tag{23}$$

where $A_0^{(1)} \equiv \varepsilon\, a_0$ and $A_L^{(1)} \equiv \varepsilon\, a_L$.

The term (23) describes the linear wave process in homogeneous, physically linear elastic material. The reflection and interaction of waves are characterized here by the linear superposition of waves.

From the point of view of NDT, it is interesting to follow the wave process in terms of the function $U_{,X}^{(1)}(X,t)$ that characterizes stress distribution in this material [8] and is plotted in Fig. 1.

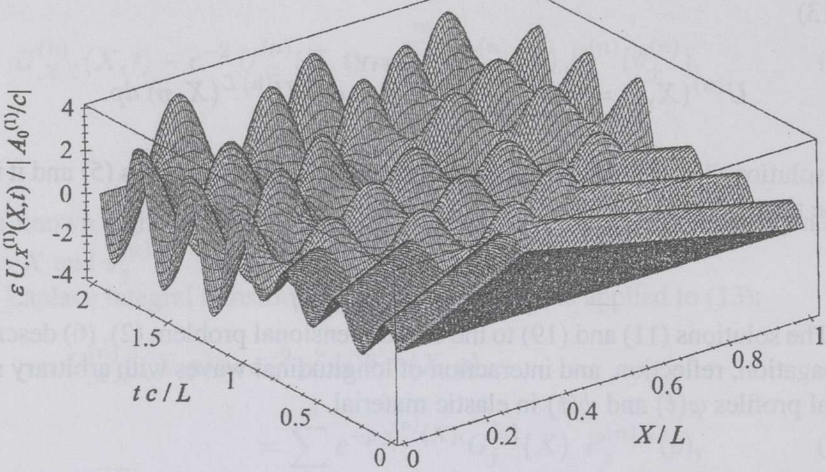

Fig. 1. Interaction of longitudinal stress waves in homogeneous elastic material.

All plots in this paper were computed making use of the following data. The density of the material $\rho_0 = 2800\ \mathrm{kg/m^3}$, the constants of elasticity $\lambda = 50$ GPa, $\mu = 27.6$ GPa, $\nu_1 = -136$ GPa, $\nu_2 = -197$ GPa, $\nu_3 = -38$ GPa, and the dimension $L = 0.1$ m. The propagation of sine waves is characterized by the frequency ω, the amplitudes $a_0 = -a_L = -c$ m/s, and by the value of the parameter $\varepsilon = 1 \times 10^{-4}$. On some plots the notation $U_{xm}^{(i)}(s,t) = \varepsilon^{(i)}\, U_{,X}^{(i)}(s,t)/\,|\,A_0^{(1)}/c\,|$, $i = 1, 2, 3,\ s = 0, L$, is used.

In Fig. 1 the wave frequency $\omega = 1.15539 \times 10^6$ rad/s. In this case the amplitude of the function $U_{,X}^{(1)}(X,t)$ in the wave interaction domain is essentially greater than the initial wave amplitudes. One possibility of using this effect in NDT is to record the function $U_{,X}^{(1)}(X,t)$ at the points $X/L = 0$ and $X/L = 1$. The plots to illustrate this are presented in Fig. 2. The amplitude amplification in the wave interaction domain is frequency dependent. The maximum amplification occurs if the number of wave periods n in the time interval $0 \le t\,c\,/\,L < 1$ is equal to the integer. On the first plot in Fig. 2 $n = 3$, which corresponds to $\omega = 1.15539 \times 10^6$ rad/s and the discussed amplification is three times. In the case of n equal to the integer and a half there is no amplification at all (the second plot in Fig. 2: $n = 3.5$, $\omega = 1.34796 \times 10^6$ rad/s). In other cases the amplification magnitude is between these two values (the third plot in Fig. 2: $n = 3.75$, $\omega = 1.44424 \times 10^6$ rad/s).

The second term in the solution (22), derived on the basis of (13)–(19) under the conditions (12), corrects the solution by introducing nonlinear effects. This term may be presented in the form of the sum

$$\varepsilon^2\, U_{,t}^{(2)}(X,t) = U_{,t}^{1(2)}(X,t) + U_{,t}^{2(2)}(X,t). \tag{24}$$

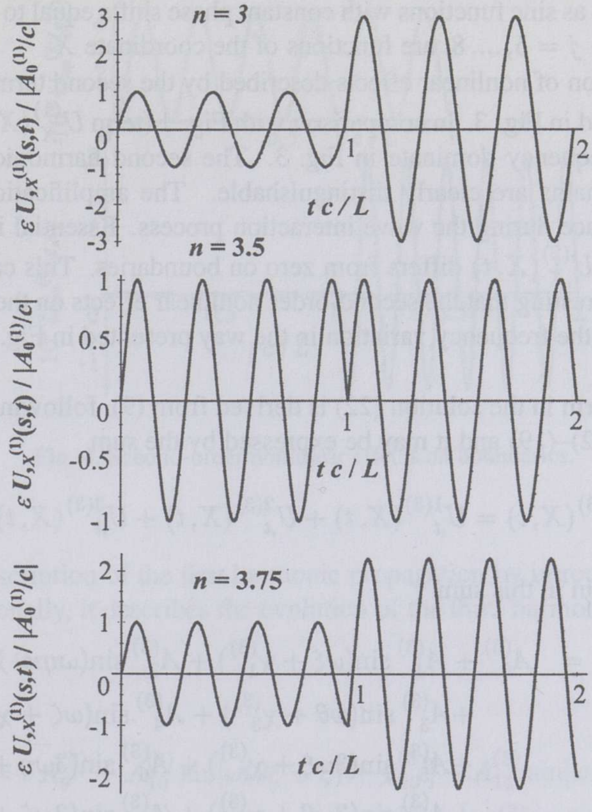

Fig. 2. Dependence of wave interaction on frequency variation.

The first constituent of this sum

$$U_{,t}^{1(2)}(X,t) = A_0^{(2)} + A_1^{(2)} \sin 2\omega\xi + A_2^{(2)} \sin 2\omega\eta$$
$$+A_3^{(2)} \sin(2\omega\theta + \chi_3) + A_4^{(2)} \sin(2\omega\zeta + \chi_4) \qquad (25)$$

contains a nonperiodic term $A_0^{(2)}$ and four terms to describe the evolution, propagation, and reflection of the second harmonic in physically nonlinear elastic material. The phase shifts of the last two terms are functions of the spatial coordinate and they are caused by the interaction between the incident and the reflected wave.

The second function $U_{,t}^{2(2)}(X,t)$ in (24) is expressed as follows:

$$U_{,t}^{2(2)}(X,t) = A_5^{(2)} \sin[\omega\,(\xi+\zeta) + \chi_5] + A_6^{(2)} \sin[\omega\,(\theta+\eta) + \chi_6]$$
$$+A_7^{(2)} \sin[\omega\,(3\zeta-\xi) + \chi_7] + A_8^{(2)} \sin[\omega\,(3\theta-\eta) + \chi_8]$$
$$+ A_9^{(2)} \cos[2\omega\,(2\theta-\eta)] + A_{10}^{(2)} \cos[2\omega\,(2\zeta-\xi)]. \qquad (26)$$

This function describes the part of the second harmonic that originates from the interaction of waves in nonlinear elastic material. The cosine functions may be considered here as sine functions with constant phase shifts equal to $\pi/2$. The other phase shifts χ_j, $j = 5, ..., 8$, are functions of the coordinate X.

The evolution of nonlinear effects described by the second term in the solution (22) is illustrated in Fig. 3. In comparison with Fig. 1 (term $U_{,X}^{(1)}(X,t)$), the effects with double frequency dominate in Fig. 3. The second harmonic evolution and interaction domains are clearly distinguishable. The amplification of nonlinear effects takes place during the wave interaction process. Essential is that the value of the function $U_{,X}^{(2)}(X,t)$ differs from zero on boundaries. This case is plotted in Fig. 4. It is interesting that the second-order nonlinear effects on the boundaries are not sensitive to the frequency variation in the way presented in Fig. 2 for the linear case.

The third term in the solution (22) is derived from (9), following the procedure described by (12)–(19) and it may be expressed by the sum

$$\varepsilon^3 U_{,t}^{(3)}(X,t) = U_{,t}^{1(3)}(X,t) + U_{,t}^{2(3)}(X,t) + U_{,t}^{3(3)}(X,t). \tag{27}$$

The first term in this sum

$$\begin{aligned} U_{,t}^{1(3)}(X,t) \;\; = \;\; & A_0^{(3)} + A_1^{(3)} \sin(\omega\xi + \chi_1^{(3)}) + A_2^{(3)} \sin(\omega\eta + \chi_2^{(3)}) \\ & + A_3^{(3)} \sin(\omega\theta + \chi_3^{(3)}) + A_4^{(3)} \sin(\omega\zeta + \chi_4^{(3)}) \\ & + A_5^{(3)} \sin(3\omega\xi + \chi_5^{(3)}) + A_6^{(3)} \sin(3\omega\eta + \chi_6^{(3)}) \\ & + A_7^{(3)} \sin(3\omega\theta + \chi_7^{(3)}) + A_8^{(3)} \sin(3\omega\zeta + \chi_8^{(3)}) \end{aligned} \tag{28}$$

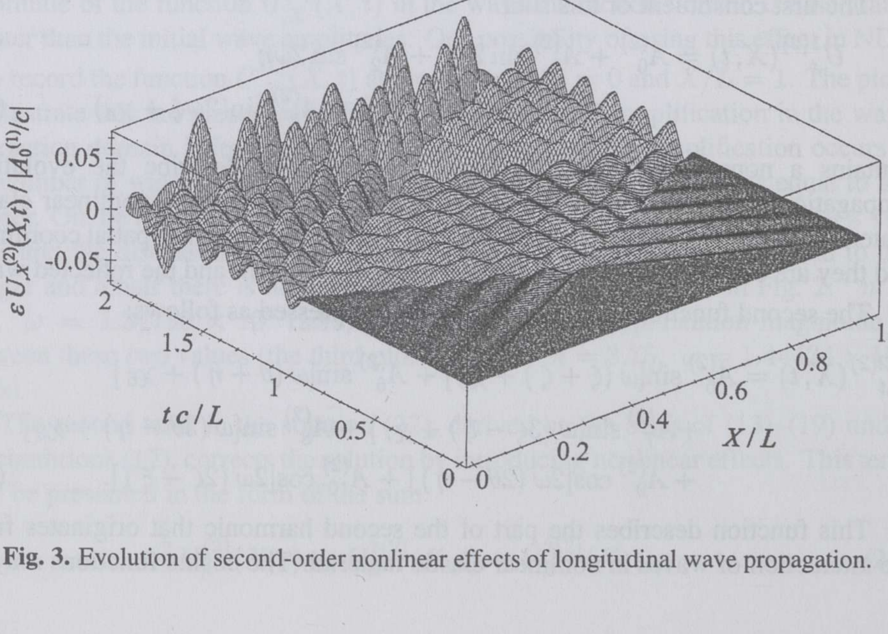

Fig. 3. Evolution of second-order nonlinear effects of longitudinal wave propagation.

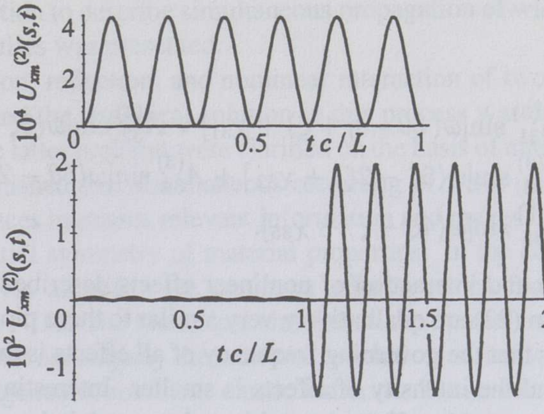

Fig. 4. Second-order nonlinear effects on boundaries.

corrects the description of the first harmonic propagation by introducing nonlinear effects. Additionally, it describes the evolution of the third harmonic.

The second term

$$\begin{aligned}
U_{,t}^{2(3)}(X,t) \;=\; & A_9^{(3)} + A_{10}^{(3)} \sin[\omega(2\xi+\zeta)+\chi_{10}^{(3)}] + A_{11}^{(3)} \sin[\omega(2\xi+\theta)+\chi_{11}^{(3)}] \\
& + A_{12}^{(3)} \sin[\omega(2\xi+\eta)+\chi_{12}^{(3)}] + A_{13}^{(3)} \sin[\omega(2\xi-\eta)+\chi_{13}^{(3)}] \\
& + A_{14}^{(3)} \sin[\omega(2\xi-\theta)+\chi_{14}^{(3)}] + A_{15}^{(3)} \sin[\omega(2\eta+\xi)+\chi_{15}^{(3)}] \\
& + A_{16}^{(3)} \sin[\omega(2\eta+\theta)+\chi_{16}^{(3)}] + A_{17}^{(3)} \sin[\omega(2\eta+\zeta)+\chi_{17}^{(3)}] \\
& + A_{18}^{(3)} \sin[\omega(2\eta-\xi)+\chi_{18}^{(3)}] + A_{19}^{(3)} \sin[\omega(2\zeta-\theta)+\chi_{19}^{(3)}] \\
& + A_{20}^{(3)} \sin[\omega(2\eta-\zeta)+\chi_{20}^{(3)}] + A_{21}^{(3)} \sin[\omega(2\theta+\xi)+\chi_{21}^{(3)}] \\
& + A_{22}^{(3)} \sin[\omega(2\theta+\eta)+\chi_{22}^{(3)}] + A_{23}^{(3)} \sin[\omega(2\theta+\zeta)+\chi_{23}^{(3)}] \\
& + A_{24}^{(3)} \sin[\omega(2\theta-\xi)+\chi_{24}^{(3)}] + A_{25}^{(3)} \sin[\omega(2\theta-\zeta)+\chi_{25}^{(3)}] \\
& + A_{26}^{(3)} \sin[\omega(2\zeta+\xi)+\chi_{26}^{(3)}] + A_{27}^{(3)} \sin[\omega(2\zeta+\theta)+\chi_{27}^{(3)}] \\
& + A_{28}^{(3)} \sin[\omega(2\zeta-\eta)+\chi_{28}^{(3)}] + A_{29}^{(3)} \cos[\omega(2\zeta+\eta)]
\end{aligned} \tag{29}$$

describes the same phenomena as the first one. The difference is that all these phenomena are caused by the interaction of various waves in different domains of the $X-t$ plane. The constituents of the function $U_{,t}^{(3)}(X,t)$, with coefficients higher than two in arguments, are collected into the third term of the sum (27)

$$
\begin{aligned}
&U_{,t}^{3(3)}(X,t) \\
&\quad = A_{30}^{(3)} + A_{31}^{(3)} \sin[\omega(3\theta - \eta + \zeta) + \chi_{31}] + A_{32}^{(3)} \sin[\omega(3\zeta - \xi + \theta) + \chi_{32}] \\
&\qquad + A_{33}^{(3)} \sin[\omega(5\zeta - 2\xi) + \chi_{33}] + A_{34}^{(3)} \sin[\omega(5\theta - 2\eta) + \chi_{34}] \\
&\qquad + A_{35}^{(3)} \sin[\omega(4\zeta - \xi) + \chi_{35}].
\end{aligned} \tag{30}
$$

The evolution and interaction of nonlinear effects described by the third term (27) in the solution (22) are qualitatively very similar to these plotted in Fig. 3. The main difference is that the governing frequency of all effects is the frequency of the third harmonic and the intensity of effects is smaller. Interesting is that the third-order nonlinear interaction effects are subjected to modulation on the boundaries (Fig. 5).

5. CONCLUDING REMARKS

This paper was stimulated by the necessity to elaborate a relatively simple method of NDT of materials with complicated properties. The main idea was to enhance the efficiency of NDT by considering instead of one propagating wave two waves excited simultaneously on the parallel surfaces of the material. Simultaneous analysis of propagation, reflection, and nonlinear interaction data of two waves increases essentially the information useful for nondestructive determination of the materials with complicated properties.

Simultaneous nonlinear propagation of two longitudinal waves in isotropic homogeneous nonlinear elastic material was considered. The algorithm for deriving

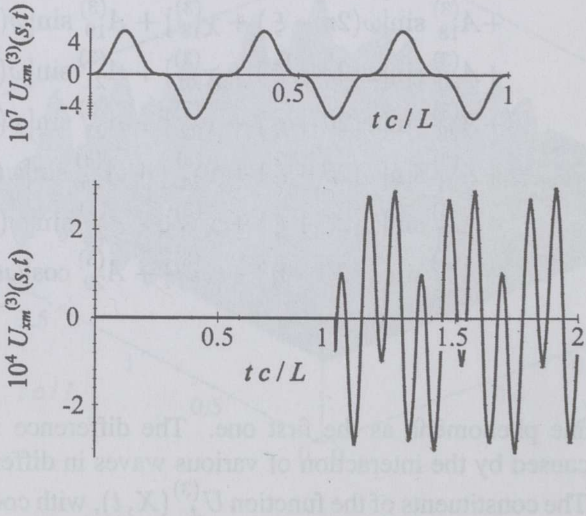

Fig. 5. Third-order nonlinear effects on boundaries.

the analytical solution to describe simultaneous propagation of waves with arbitrary smooth initial profiles was presented.

The propagation, reflection, and nonlinear interaction of two sine waves were studied in detail and the analytical solution to this process was derived. The basic peculiarities of the latter problem were clarified on the basis of numerical simulation data. It was established that simultaneous recording of wave propagation data on two opposite surfaces increases relevant information and makes it possible to easily determine the spatial symmetry of material properties. In the considered case the interaction of waves amplifies the nonlinear effects, which facilitates utilization of these effects in NDT. The numerical simulation data presented characterize the specific features that accompany the harmonic evolution, reflection, and interaction in isotropic homogeneous nonlinear elastic material. These data may be regarded as reference data for solving more complicated NDT problems.

ACKNOWLEDGEMENT

The support of the Estonian Science Foundation (grant 3131) is gratefully acknowledged.

REFERENCES

1. Truell, R., Elbaum, C. and Chick, B. B. *Ultrasonic Methods in Solid State Physics.* Academic Press, New York, 1969.
2. Pao, Y.-H., Sachse, W. and Fukuoka, H. Acoustoelasticity and ultrasonic measurements of residual stresses. In *Physical Acoustics* (Mason, W. P. and Thurston, R. N., eds.). Academic Press, Orlando, 1984, **17**, 61–143.
3. Bhardwaj, M. C. Fundamental developments in ultrasonics for advanced NDC. In *Nondestructive Testing of High-Performance Ceramics. Conference Proceedings.* American Ceramic Society, Inc. Westerwille, Ohio, 1987, 472–527.
4. Takuoka, T. Weak and short waves in one-dimensional inhomogeneous nonlinear elastic materials. *J. Acoust. Soc. Am.,* 1981, **69**, 66–69.
5. Ravasoo, A. Ultrasonic nondestructive evaluation of inhomogeneous plane strain in elastic medium. *Res. Nondestr. Eval.,* 1995, **7**, 55–68.
6. Nigul, U. K. *Echo-Signals from Elastic Objects*, Vol. 1. Valgus, Tallinn, 1976 (in Russian).
7. Engelbrecht, J. K. and Nigul, U. K. *Nonlinear Deformation Waves.* Nauka, Moscow, 1981 (in Russian).
8. Eringen, A. C. *Nonlinear Theory of Continuous Media.* McGraw-Hill, NewYork, 1962.

PIKILAINETE MITTELINEAARNE INTERAKTSIOON ELASTSES MATERJALIS

Arvi RAVASOO ja Andres BRAUNBRÜCK

Teoreetiliselt on uuritud pikilainete mittelineaarset interaktsiooni füüsikaliselt mittelineaarsete omadustega elastses materjalis. On tuletatud analüütiline lahend materjali paralleelsetel vastaspindadel samaaegselt tekitatud kahe pikilaine levi kirjeldamiseks. Põhjalikult on vaadeldud siinuslainete levi ja interaktsiooni ühemõõtmelises seades. Numbriliste arvutuste tulemuste alusel on välja selgitatud siinuslainete levi ja peegeldusega kaasnevate mittelineaarsete nähtuste evolutsiooni ja interaktsiooni iseärasused.